

# POLYMERIC ABLATION INDUCED BY FREE BURNING ARCS IN AIR

M. BATOR\*, R. BIANCHETTI, P. SUETTERLIN

ABB Corporate Research Center Switzerland, Segelhofstrasse 1K, 5405 Baden-Daettwil, Switzerland

\* matthias.bator@ch.abb.com

**Abstract.** We investigate the influence of switching arcs on different polymers and their interaction. We describe a set of experiments on a simplified model geometry typical for low voltage switchgear. In a broad range of experimental conditions and parameters such as arc current, polymeric material or contact material, the voltage, the mass loss and the corresponding pressure build-up are examined. From this raw data, we deduce the arc influence on the ablation process as well as the feedback on some arc plasma properties.

**Keywords:** free burning arcs, low voltage switchgear, plasma properties, polymeric ablation, thermoplastics.

## 1. Introduction

Low voltage switchgear and the corresponding development processes matured over decades and today are highly optimized. Thus, most development often concentrates on optimization of very specific details such as arc chamber geometries, contact materials and very often the exact composition of plastic parts. Interestingly, when testing new polymers, the approach is often to test a wide range of materials and settle with the best as the understanding of the underlying interaction between the arc and ablated polymers is often lacking.

The goal of the investigation presented in this paper is to improve exactly this understanding. Two simplified laboratory setups were used, one with two parallel polymeric plates with an arc ignited between two cylindrical electrodes, and the other with a polymeric cylinder in order to constrict the arc axially. We investigated the mass loss, the arc voltage and the pressure build up in dependence on the current as well as the polymeric and contact material. Specifically PA6, PA66, PTFE and PE were investigated in pure forms as well as containing additives. The electrodes consisted of either copper or steel.

## 2. Experimental Setup

The setup consisted of a capacitor bank with 32 mF charged up to 950 V. It was discharged through an inductance and the DUT (device under test) with a pseudo 50 Hz pulse. A second variation used an additional buck converter allowing for an actively controlled current discharge of the capacitor through our DUT (see Figure 1). In these cases, the capacitor bank was used in a 16 mF configuration and was typically charged up to 1600 V. Two different geometries (see were used with both setups.

In the setup including the buck converter, current control was achieved by switching an ABB HiPak IGBT via a feedback PI control (see Figure 1). As

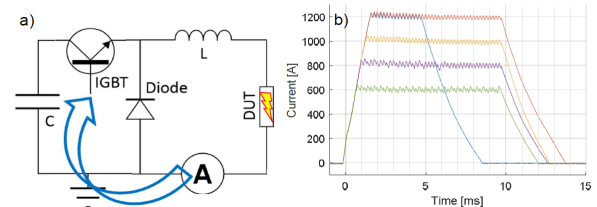


Figure 1. a) Schematics of the active current control setup. A pre charged capacitance ( $C$ ) is discharged via an IGBT and an inductor ( $L$ ) through the DUT. The current ( $A$ ) is used to control the semiconductor. b) Currents (0.6, 0.8, 1.0 and 1.2 kA) set using the setup in a). In one instance, the control loop was stopped after 5 ms; the others were stopped after 10 ms.

long as the current was below the set value, the IGBT was on and the current rose with a time determined by the used inductance (1.5 mH in our case) and the voltage difference between arc and the capacitor bank. After reaching the set current, the ABB HiPak IGBT is switched off and the current decreases as energy is dissipated in the arc. As a result, a small ripple (determined by amongst others the inductance and the control frequency) is visible on the current trace, which typically was in the range of  $\pm 20$  A on a 1 kA set current. Either after a set time or when the capacitor voltage drops below the voltage of the DUT no modulation of the current occurs and it drops to zero.

### 2.1. Parallel Plate Geometry

As mentioned, two different geometries were used as DUT, both utilizing a thin wire for ignition. In the first, two polymeric plates were arranged in parallel with one electrode mounted on the right between the two plates (see Figure 2) allowing for optical access from the side perpendicular to the arc direction. The second electrode is mounted to the left of the plates just outside the picture shown in Figure 2. The plate surface measures 20 x 40 mm with an adjustable distance in this case set to 12 mm. This setup resem-

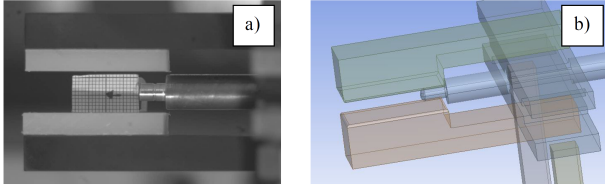


Figure 2. a) Side view of the parallel plate geometry. An electrode is mounted on the right between the two polymeric plates to be investigated. The second electrode, on axis with the first is not shown on the left side. The plates were separated by 12 mm. b) CAD model of the geometry.

bles the typical configuration present in a low voltage breaker with an arc squeezed in between two polymeric walls.

## 2.2. Nozzle Type Geometry

In the second geometry, a tube replaced the polymeric plates. Here, the electrode is mounted gastight inside the tube on the right (see Figure 3) such that gas flow is only allowed towards the left. The second electrode is again mounted outside of the polymeric region (visible on the left side of Figure 3 a)). The channel within the tube has a length of 45 mm with a variable inner diameter of 5, 7 or 10 mm. The closed geometry allows for an additional pressure measurement inside the tube. Differently to the parallel plate setup, optical access is only given at the outlet of the tube and no longer along the whole arc.

## 2.3. Optical Measurements

A high-speed camera setup is arranged perpendicular to the arc direction in order to visualize the plasma under different conditions. Typical exposure times were in the range of a few  $\mu\text{s}$ . This allowed to either visualize a detailed time evolution of the plasma or give a good overview of its distribution. Using bandpass filters allowed to better distinguish emission from specific sources such as the  $H_\alpha$ - or specific metallic lines.

## 3. Results

The two setups were used to investigate different aspects of the polymer-arc interaction. The parallel plate setup was used to optically investigate the spatial distribution of the arc and how it is influenced by degassing of the polymers. In the cylindrical setup, we concentrated on the pressure and arc voltage build-up during the arcing as well as on the integrated mass loss of the polymeric tubes.

### 3.1. Plasma Distribution

The main interest of the investigation was the interaction of the plasma with the polymeric walls. In a first step, we investigated how the arc arranges itself within the parallel polymeric plates. This is done by doing time-resolved optical imaging of the arc using

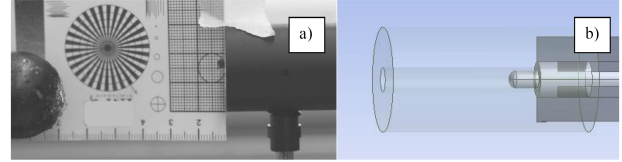


Figure 3. a) Side view of the nozzle geometry. An electrode is mounted on the right inside a hollow polymeric cylinder. The right side is designed to be air tight, while the left is open towards the ground electrode (also shown). b) CAD model of the geometry. The electrode tip has a diameter of 5 mm.

the high-speed camera. In a first series, neat PA6 (neat in this context meaning commercially available pure compounds) plates were arranged 12 mm apart. The applied current was a pseudo 50 Hz pulse with 3 kA peak value.

The ignition wire explodes ca. 0.1 ms after current initiation filling the volume in front of the contact with hot metallic plasma and residues of the wire. In this early phase, up to ca. 0.5 ms (see Figure 4, left column), the hot plasma is distributed asymmetrically and touches the polymeric walls (within our resolution of ca. 0.1 mm). The behavior changes quickly as the current increases; the arc becomes brighter and more constricted. After ca. 1.5 ms, the arc generally stabilizes into a symmetric, constricted shape with dark regions between the bright center and the polymeric walls. In all measurements, a sharp edge between the central arc plasma and the dark region around it is observed. A light glow is visible at the polymeric walls (see Figure 4 left column 5.0 ms). Optical emission spectroscopy results (not discussed in this paper in detail) show that the spectral distribution in this region is identical to the center of the arc comprising mostly ionized metal lines. This leads to the conclusion that the light is most likely reflected and/or scattered from

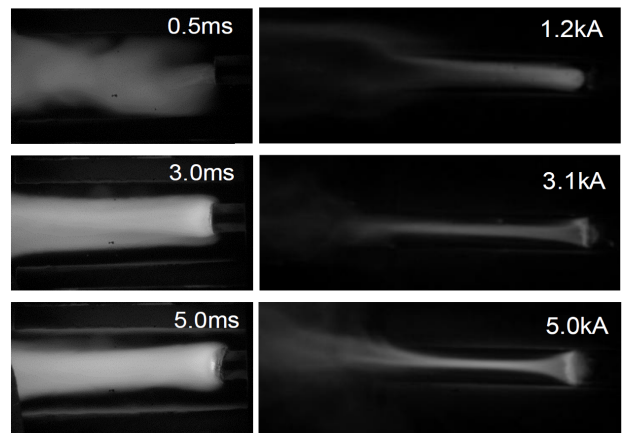


Figure 4. Left panel: Time sequence of a single discharge with neat PA6 walls and a 50 Hz discharge with a 3 kA peak current. Right panel: High-speed frames of an arc discharge with copper electrodes using a band-width filter at 514.5 nm (3 nm FWHM) exposed for 4  $\mu\text{s}$  at peak current. The walls used are neat PTFE.

the central arc and not emission from evaporating polymers. The exact shape of the arc is not determinable in this setup due to the camera axis being centered between the plates and perpendicular to the arc direction. We assume that the initially cylindrical arc is squeezed into a flattened distribution between the plates.

With changing current and polymeric material, the general behavior does not change. In all measurements, the arc becomes more constricted in the center region, and most likely distributes wider along the optical axis of the camera with increasing currents as shown in Figure 4 (right column). These pictures were taken with an additional bandpass filter around 514.5 nm with a width of 3 nm to enhance the observed radiation coming from atomic emission lines of copper. Furthermore, the wall material in this column is PTFE and not PA6 as in the images on the left. Interestingly, no emission is observed between the polymer and the bright arc regardless of the current. Even additional spectroscopy and absorption measurements (not presented here) do not allow for a classification of the "dark zone" between the polymeric walls and the central arc. A disadvantage of the parallel plate setup and in particular the open sides along the optical axis is the build-up of free-floating fumes in front of the plasma as can be observed towards the top left of the 5.0 kA high speed picture in Figure 4. It covers the plasma, as well as the dark region and therefore falsifies the optical impression of the distance of the arc to the polymeric walls. This effect is considerably stronger using PA6 walls.

The two take-away observations are that the polymer gases are optically not accessible due to most likely being too cold to generate radiation. And secondly that a strong spatial constriction of the arc is observed which considerably increases with higher currents and therefore larger degassing of the polymer.

### 3.2. Mass Loss and Pressure Build-up

In the second set of experiments, using the nozzle setup, the arc constriction was as apparent as before. At the nozzle opening, the bright plasma region in the center was surrounded with a dark region towards the walls of the polymeric tube. Still, using this setup the focus of the investigations shifted from the optical investigation to the pressure build-up and voltage during the arcing as well as the mass loss of the polymer tube.

The pressure build-up is an important indicator for the interruption process as the ablated polymers interact in complex ways with the arc. In general, it is considered advantageous to increase the amount of ablated polymer mostly due to its effect of cooling the arc and thus leading to higher arc voltages. Furthermore, the flow can be used either to control the movement of the arc or to diffuse the arc in specific nozzle configurations. Depending on the exact polymeric material used, an additional benefit is the

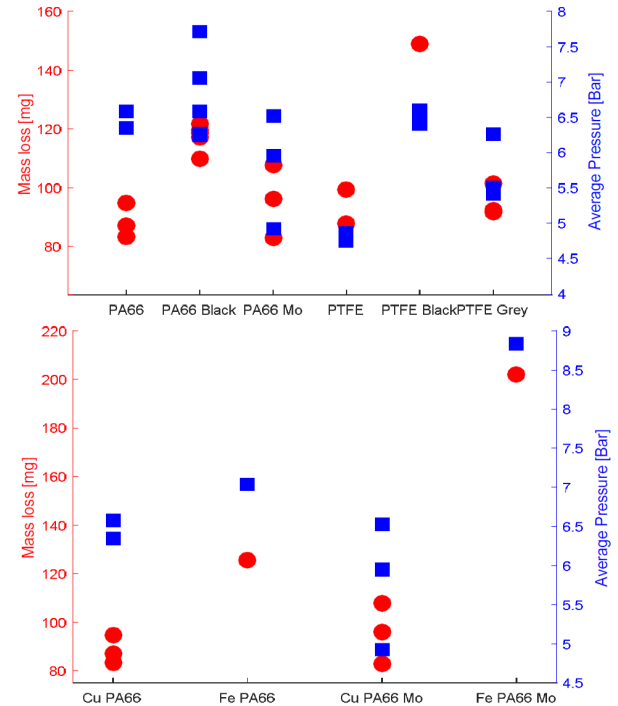


Figure 5. Measured total mass loss (red circles, left axis) and average pressure build-up (blue squares, right axis) for different nozzle materials using a controlled 1.2 kA discharge during 10 ms and different material combinations.

reduced conductivity compared to a metallic plasma and a possibly higher dielectric stability after current zero. Still, there are also disadvantages related to a large amount of hot polymeric gases. Too high pressures might lead to an explosive destruction of the device, in particular at higher currents when the outgassing is scaled up by the current. Furthermore, some polymeric materials, such as e.g. PTFE can lead to higher conductivity in regions with large concentrations [1] leading to either re-strikes outside of the arc chamber during the interruption or to re-ignitions after current zero.

Therefore, it is often necessary to take the decision for a polymeric wall material on a per-device base leading to additional work and uncertainties in the development process. A better understanding of the ablation process on a very general base would help to reduce the necessary testing and ideally enable a better predictability of polymer choices.

In the following we will discuss the findings using combinations of copper, steel, and silver electrodes with neat PA66, "black" PA66 (PA66 with <1% of carbon black), neat PTFE, "grey" PTFE (PTFE with molybdenum disulfide), neat PE and "black" PE (all commercially sourced). The findings are shown in Figure 5. The top panel shows the mass loss and average pressure for different polymers using copper electrodes, while the bottom panel compares PA66 and "black" PA66 using copper and steel electrodes. In both cases, we did not use a 50 Hz discharge, but a

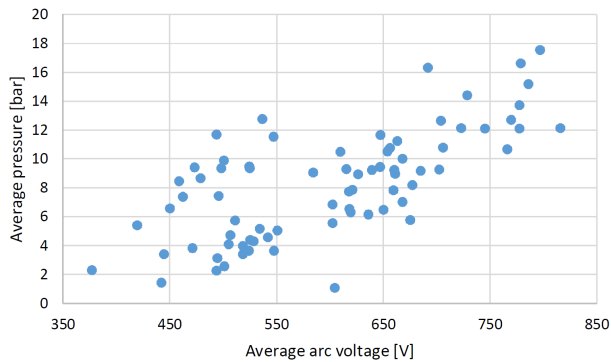


Figure 6. Measured average pressures versus averaged arc voltage in all recorded discharges using the nozzle type setup and the 50Hz synthetic circuit.

controlled 10 ms long current (as shown in Figure 1). The values are averaged between 3 and 8 ms where the variation is the lowest and the influence of the ignition process is no longer present.

We observe a clear trend towards higher ablation ratios for the "black" and "grey" variants of PA66 and PTFE. It has to be mentioned that the spread in identical measurements could be explained by slightly leaky arrangement in particular after several shots when the inner diameter widened slightly. Carbon black is typically used to enhance stability versus UV radiation [2]. Due to the high temperatures in the arcing plasma, usually more than 50% of the radiation reaching the polymeric walls has a wavelength below 300 nm [3]. A stronger absorption in the top-most layers therefore leads to an increase of the ablation processes. Similarly, the higher ablation when using steel electrodes can be explained. The higher net emission compared to copper [4] would result in a larger amount of radiation reaching the walls and thus lead to larger ablation. Furthermore, more ablated metal in addition can change the interaction with the polymeric walls. Interestingly, the pressure in PA66 stays mostly the same for neat PA66, black PA66 and PA66 Mo, while the mass loss is measurably higher for the black version. A possible explanation is that this comparison only includes ablation into the gaseous phase, while the generation of particles and droplets, which can strongly vary between different polymers, typically has less influence on the plasma properties but strongly influences the mass loss. Hence, one could assume that in the case of the black PA66 the stronger absorption leads to a slight increase in gaseous ablation but a stronger increase in generation of particles and droplets. Comparing PTFE and black PTFE on the other hand shows a measurable increase in both, the mass loss and the average pressure. Therefore, in this case one can conclude that the higher absorption is a more direct translation into a larger generation of polymeric gas.

In order to observe the general correlation between the pressure and arc voltages, all measurements using a 50 Hz discharge are shown in Figure 6. The values

are taken at the peak currents, but include all material combinations as well as different current settings. Even considering this wide variety and the findings discussed before, a general linear trend is observed. Placing an additional floating electrode at the exit of the nozzle we found that ca. 60-70% of the voltage drop appears in the nozzle. In order to explain the increase of the arc voltage with the pressure, we have to consider the findings from the parallel plate setup regarding how the current influences the arc shape and the extent of the dark layer dominated by relatively cold polymeric gases. The increase of the current leads to higher ablation rates and therefore higher pressures. At the same time, the hotter arc is being constricted in a smaller space. The electrical conductivity is very low at temperatures below 5 kK, grows linearly until ca. 20 kK where it finally flattens out [5]. Therefore, the slightly higher temperature in the core of the arc is not able to compensate the exponentially lower conductivity in the dark regions of "cold" polymer gases leading to an increase of the arc voltage in conditions where a high pressure is expected.

## 4. Conclusions

We investigated the interaction between polymeric ablation and an electrical arc. We could clearly show the influence the ablated polymer has on the shape of the arc and its flow patterns. Furthermore, we could show how dominant the dark region of relatively cold polymeric gases is not only on the shape but also on the electrical properties of the arc, in particular the arc voltage. Together with the findings that the ablation of polymers can be significantly increased using compounds that incorporate e.g. carbon black the results can be used to further optimize prediction models in switchgear development. The differences in ablation when using steel electrodes compared to copper electrodes further show that the influence of the splitter plates in a real breaker on the ablation properties should not be neglected.

## References

- [1] Y. Okano et al. Quenching performance of air arc discharge with polymer insulators. *20th Int. Conf. on Gas Disch. and Their Appl.*, 745(A39):199–202, 2014.
- [2] R.J. Young and P.A. Lovell. *Introduction to Polymers*. Third Edition. CRC Press, 2011.
- [3] ABB. Internal communication/publication.
- [4] Y. Cressault and A. Gleizes. Thermal plasma properties for Ar-Al, Ar-Fe and Ar-Cu mixtures used in welding plasma processes: I. net emission coefficients at atmospheric pressure. *J. Phys. D: Appl. Phys.*, 46:415206, 2013. doi:10.1088/0022-3727/46/41/415206.
- [5] S. Franke et al. Temperature determination in copper-dominated free-burning arcs. *J. Phys. D: Appl. Phys.*, 47:015202, 2014. doi:10.1088/0022-3727/47/1/015202.